Investigation on Rotation/Curvature Correction Methods of SST Turbulence Model in Numerical Simulation of Axial Compressor

Ziwei Wang, Jie Cao, Xuejiao Jing, Baiyu Li, Bin Li*

Computational Aerodynamic Institution, China Aerodynamics Research and Development Center, Mianyang, China

* Corresponding Author Email: 45241968@foxmail.com

Abstract. Turbulence models which are widely used in engineering applications usually need correction in axial compressor CFD simulations due to the intense rotation of the system. In order to understand the applicability of rotation-curvature correction methods of turbulence models in numerical simulation of axial compressors, several correction methods were implemented based on SST turbulence model on an inhouse CFD solver ASPAC and numerical simulations were carried out on a transonic compressor Rotor37. The results shows that the rotation/curvature correction models mainly affect the corner separation on the suction surface of the blade. More specifically, SST-Helicity model reduces corner separation at the suction surface and performs well at conditions with relatively large mass flow rate. Results from SST-CC and SST-Hellsten model are close to but slightly worse than that of standard SST model in terms of agreement with experimental data. In summary, detailed assessment and discussions on different rotation/curvature corrections of turbulence models were carried out based on numerical results of a transonic compressor in this paper, which may contribute to the choice of turbulence models and investigation of turbulence modeling and model correction methods in axial compressor simulations in the future.

Keywords: Axial compressor, numerical simulation, computational fluid dynamics.

1. Introduction

The compressor, as one of the important components of the aero-engine, achieves the compression of the inlet air through the work done by the blades. Higher pressure ratio and compression efficiency has been the development direction of the compressor, which has a direct impact on improving engine thrust and reducing fuel consumption. Due to the prevalence of complex flow phenomena such as shock boundary layer interference, rotor tip leakage, wake interference of upstream blade row and blade stall in the compressor, it is difficult to fully obtain the flow field details through experimental studies; at the same time, experimental studies of compressors are also characterized by high cost and long lead time. In recent years, due to the development of computer hardware and numerical solution methods, CFD methods are increasingly used in the study of compressors with relatively low cost and short cycle time. At present, CFD, experimental studies and theoretical analysis have become the three main complementary tools in compressor development.

Accurate prediction of turbulence is difficult due to the non-constant high-frequency pulsations in turbulent motion and the multiplicity of spatial scales. The predictive capability of turbulence models is challenged by the compressible turbulent motion with inverse pressure gradient in a pressurized airplane and the complex flow phenomena such as separation, surge and wake disturbance. Shabbir [2] et al. used B-L, k-ε and a rotationally modified k-ε model to solve for Rotor37 and did a detailed comparison analysis with the experimental results and found that the modified k-ε model could achieve relatively good prediction results, but the three models still have large deviations in the vicinity of the hub and the wake region. Also for the transonic compressor rotor Rotor37, Yin Song et al [3] used the self-developed CFD solver to solve the SA, k-ε, and k-ω turbulence models, respectively, and the final results showed that the k-ω model had a higher accuracy of the solution junction. Liu et al [4] used Fluent to conduct a detailed analysis of the corner separation of the low-speed PVD compressor blade grille. Separation) was studied numerically in detail, comparing the

predictions of the RANS models including SA, standard k-ε, realizable k-ε, k-ω, and SST, and the Reynolds stress model for the corner separation of the suction surface. The predictions of the k-ε and Reynolds stress models were found to be in better agreement with the experiments, and the corner separation of the SA and SST models was overpredicted. Suder et al [5] carried out a detailed analysis of the transonic compressor rotor tip leakage by experimental and numerical methods, and found that the interaction between the excitation wave in the channel and the tip leakage extended the influence region to 10% of the spreading position near the magazine; and the tip leakage caused the flow channel partially blocked, increasing the angle of attack of the blade and triggering the separation of the attachment layer of the blade tip under specific operating conditions.

In addition, the flow in the compressor has a significant feature: the centrifugal and Coriolis forces have a significant impact on the flow field and turbulence generation because of the rotation of the system and the bending of the blade channels. It is shown that the bending of the flow lines in the flow field due to the rotation of the system or to the geometry of the flow channel causes an intensification or suppression of the turbulent motion in different regions of the flow field. Therefore, the vortex-viscosity model based on the assumption of isotropic turbulence is not well adapted to the turbulence calculation under the influence of flow line bending and system rotation, and it is necessary to make corrections.

The results of numerous experimental and DNS studies have shown that the Cohen's force, brought by the rotation of the system, increases the turbulent kinetic energy and turbulent shear stress at the pressure surface, but the turbulence generation at the suction surface is suppressed and thus tends to laminarize [6]-[9]. For the effect of flow line bending on turbulence, researchers have conducted extensive experimental and numerical studies based on bends [10]-[12] and found that for the vicinity of the convex surface (Convex Surface) turbulent pulsations are suppressed under the effect of vertical wall pressure gradient; while near the concave surface (Concave Surface), turbulent pulsations are intensified.

Based on the above review, it is evident that due to the complexity of the flow in a compressor, no single RANS turbulence model has yet shown significant advantages in predicting all compressor types and various specific flow phenomena. In addition, the study of the mechanism of the effect of rotation/curvature on turbulence generation and the validation of the correction model are almost always obtained based on simple rotating channels and U-tubes, and the study of the applicability of the relevant correction model in the simulation of the compressor flow is still relatively rare. Based on the energy back-transfer mechanism, Liu et al [13] proposed the SST-Helicity model, and the prediction results of the SST-Helicity model for the pressure coefficient, streamline distribution, and corner separation on the blade surface in the simulation of the PVD leaf grille are in good agreement with the experimental and Reynolds stress models, which improves the model prediction accuracy. Smirnov et al [14] proposed the SST-CC modified model and used in the simulation of centrifugal presses, and the results showed that the SST-CC model predicted better than the SST model in most operating conditions, but the effect of the modified model on the flow structure was not discussed in detail.

Although several rotational curvature correction methods based on the SST model have been proposed, the predictive capability of these correction methods in axial compressor flow simulations and the effects on the flow field details have not been fully discussed. Therefore, a systematic study of the applicability of SST model-based rotational curvature correction methods in compressor simulations is of great importance. On the one hand, it lays the foundation for understanding the complex flow mechanism in the compressor simulation, and also supports the selection of turbulence models and the turbulence modeling adapted to the compressor simulation. In this paper, three correction methods, SST-CC, SST-Hellsten and SST-Helicity, are used to study the SST turbulence model in compressor flow simulation based on the self-developed solver, and the results of the standard SST turbulence model and various correction models are analyzed and compared in detail with experimental data to investigate the effects of different turbulence model correction methods on

the compressor The prediction ability of different turbulence model modification methods on the overall performance and flow field details of the compressor is investigated.

2. Computational Method

2.1 Numerical Method

In this paper, ASPAC [15] [16], a three-dimensional structured grid solver independently developed by our research group, is used to solve dimensionless NS equations in Cartesian coordinate system.

$$\frac{\partial}{\partial t}\int_V \vec{W} dV + \iint_S \left(\vec{F_c} - \vec{F_v}\right)\cdot d\vec{S} = \iint_S \vec{S_T} d\vec{S} \tag{1}$$

where V is the control volume, S is the surface of the closed control body, and $\vec{W}$ is a vector consisting of conserved variables. $\vec{F_c}$ and $\vec{F_v}$ are the convective and viscous fluxes; $\vec{S_T}$ is the source term containing the centrifugal and Coriolis forces. The convective flux is discretized by using the Roe scheme of flux difference splitting, in which the left and right values of the flow field variables are obtained by MUSCL interpolation. Second order central difference is used for viscous flux. The time discretization is in the implicit format with LU-SGS iterative advance.

2.2 Physical Model

Rotor37 is an imported rotor developed by NASA Lewis Laboratory in the axial flow compressor project for suction engines. The number of blades in the whole turn is 36, the design speed is 17188.7 rpm, and the main characteristic parameters of Rotor37 are shown in Table. 1 [17]. Reid and Moore [18] carried out detailed experimental measurements on the inlet stage of the compressor including Rotor37.

In order to reduce the computational mesh size, only one blade channel was taken for the Rotor37 calculation and a hexahedral structured mesh was generated for the constant solution. The top clearance of 0.0356 cm at the top of the blade is retained in the model.

Table 1. Rotor37 design parameters.

Parameters	Pressure ratio	Adiabatic efficiency	Rotor tip speed $/\,\mathrm{m}\cdot\mathrm{s}^{-1}$	$\dot{m}_{choke}/\mathrm{kg}\cdot\mathrm{s}^{-1}$	$\dot{m}_{NS}/\dot{m}_{choke}$
	2.106	0.877	454.1	20.93	0.925

Simulations were carried out at the design speed. The inlet is given the Station 1 total temperature and total pressure distribution as well as the axial inlet conditions provided in the literature [17] in the spreading direction; the spatial periodic boundary conditions are used on both sides of the passage; the outlet is set up as a pressure outlet, given the static pressure at the hub and the static pressure distribution in the outlet radial direction is obtained by the radial balance equation. By gradually increasing the outlet pressure, the characteristic curve of the compressor is obtained by simulation.

2.3 Computation Grid

In this paper, a detailed grid-independence check is carried out, and the final number of grid cells used is 1.97 million. In order to ensure the accuracy of the flow solution in the boundary layer, the height of the first grid layer is 1×10-6 m. The grid schematic is shown in Fig. 1.

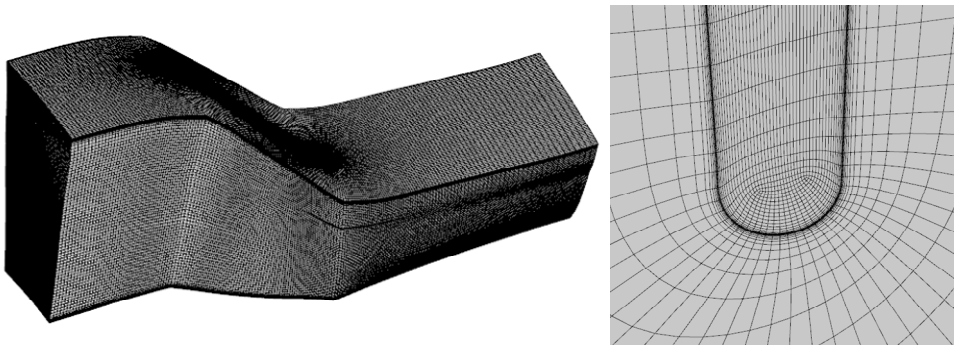

(a) (b)

Figure 1. (a) Computation grid for Rotor37; (b) grids in the tip gap.

3. Turbulence Models and Modification Methods

3.1 SST Turbulence Models

The SST turbulence model was proposed by Menter [19]. The model combines the k-ω turbulence model and the k-ε turbulence model, which is solved directly using the k-ω model in the viscous bottom and logarithmic domains, avoiding the use of wall functions; in the outer boundary layer region (wake region) and the mainstream region, the k-ε solution is used, circumventing the problem that the k-ω model is overly sensitive to the mainstream ω values [20]. The SST turbulence model obtains the turbulent viscosity by solving the turbulent kinetic energy k and the transport equation for the turbulent specific dissipation rate ω to obtain the turbulent viscosity:

$$\frac{\partial(\rho k)}{\partial t} + u_j \frac{\partial(\rho k)}{\partial x_j} = P - \beta' \rho k\omega + \frac{\partial}{\partial x_j}\left[(\mu + (\frac{\mu_T}{\sigma_k}))\frac{\partial k}{\partial x_j}\right] \tag{2}$$

$$\frac{\partial(\rho\omega)}{\partial t} + u_j \frac{\partial(\rho\omega)}{\partial x_j} = \frac{\gamma}{\upsilon_t} P - \beta\rho\omega^2 + \frac{\partial}{\partial x_j}\left[(\mu + (\frac{\mu_T}{\sigma_\omega}))\frac{\partial\omega}{\partial x_j}\right] + 2(1-F_1)\sigma_{\omega 2}\frac{\rho}{\omega}\frac{\partial k}{\partial x_j}\frac{\partial\omega}{\partial x_j} \tag{3}$$

The turbulent viscosity coefficient is obtained by the following equation:

$$\mu_t = \min(\frac{\rho k}{\omega}, \frac{a_1 \rho k}{\Omega F_2}) \tag{4}$$

The terms on the right side of the medium sign of the turbulent energy transport equation (2) are the turbulent energy generation source term, the dissipation term and the diffusion term, respectively. Similarly, the terms on the right side of the medium sign of the specific dissipation rate equation (3) are the generated source term, the dissipation term, the diffusion term and the cross-diffusion term. Among the generating source terms:

$$P = \mu_t S^2 - \frac{2}{3}\rho k\delta_{ij}\frac{\partial u_i}{\partial x_j} \tag{5}$$

Other model parameters can be found in the literature [19] and are not described in detail here. listed in detail here.

3.2 SST turbulence model Rotation/curvature correction model

3.2.1. SST-CC correction.

Smirnov et al [14] corrected the generating source terms of the turbulent kinetic energy and turbulent specific dissipation rate equations of the SST model by identically introducing two dimensionless parameters r^* and $\tilde{r}$ to characterize the effects of curvature and rotation effects, respectively. The SST-CC correction set a correction upper limit of 1.25:

$$f_{r1}\left(r^*,\tilde{r}\right)=\left[1-c_{r3}\tan^{-1}\left(c_{r2}\tilde{r}\right)\right]\times\left(1+c_{r1}\right)\frac{2r^*}{r^*+1}-c_{r1} \tag{6}$$

$$f_{r1}=max(min(f_r,1.25),0) \tag{7}$$

The dimensionless parameters r^* and $\tilde{r}$ characterizing rotation and curvature in the SST-CC correction are defined as:

$$r^*=\frac{\sqrt{2S_{ij}S_{ij}}}{\sqrt{2\Omega_{ij}\Omega_{ij}}} \tag{8}$$

$$\tilde{r}=\frac{2\Omega_{ik}S_{jk}}{D^4}\left(\frac{DS_{ij}}{Dt}+\left(\varepsilon_{imn}S_{jn}+\varepsilon_{jmn}S_{in}\right)\Omega_m^{rot}\right) \tag{9}$$

$$D^2=max\left(2S_{ij}S_{ij},\ 0.09_{\omega^2}\right) \tag{10}$$

$$c_{r1}=1.0,c_{r2}=2.0,c_{r3}=1.0 \tag{11}$$

Where Ω_m^{rot} is the rotational angular velocity of the system, ε_{ijk} is the Levi-Civita operator of coordinate rotation, S_{ij} is the turbulent strain rate tensor.

3.2.2. SST- Helicity correction.

The Helicity correction for the SST turbulence model was proposed by Liu et al [13] to multiply the generating source terms of the turbulent kinetic energy and specific dissipation rate equations by the Helicity correction term:

$$P=\mu_t(1+C_{h1}h^{C_{h2}})S^2 \tag{12}$$

The model constants are $C_{h1}=0.71$ and $C_{h2}=0.60$ respectively. The Helicity relative density is defined as:

$$h=\frac{\left|\vec{\boldsymbol{u}}\cdot\vec{\boldsymbol{\omega}}\right|}{\left|\vec{\boldsymbol{\omega}}\right|\cdot\left|\vec{\boldsymbol{u}}\right|} \tag{13}$$

3.2.3. SST- Hellsten correction.

The SST-Hellsten correction method [21] multiplies only the dissipation term of the specific dissipation rate equation by the correction function F_4, with $C_{rc}=3.6$ as the model constant.

$$F_4=\frac{1}{1+C_{rc}R_i} \tag{14}$$

Where R_i is Richardson number,

$$R_i=\frac{|\Omega_{ij}|}{|S_{ij}|}\left(\frac{|\Omega_{ij}|}{|S_{ij}|}-1\right) \tag{15}$$

4. Results and discussion

Firstly, the predictive ability of the correction methods in the compressor flow simulation is discussed in detail by comparing the solution results of the standard SST model and various correction models on the standard model of Rotor37 with the experimental results, and the effects of various correction methods on the flow in the compressor are analyzed.

The results of solving the SST model and its correction method for the total pressure ratio and total temperature ratio of Rotor37 are shown in Fig. 2 and Fig. 3. From the total pressure results, it can be seen that the calculated total pressure value of the SST-Helicity model is large, and the overall

agreement with the experimental results is better among all models; the total pressure of the SST-CC and SST-Hellsten models is slightly lower than that of the standard SST model.

The total temperature is similar to the total pressure results: the total temperature of the SST-Helicity model is larger compared with the calculated results of the standard SST model; the total temperature values of the SST-Hellsten and SST-CC correction methods are slightly lower than those of the standard SST model, and both agree well with the experimental values.

It is also noteworthy that the SST-Hellsten model is more difficult to obtain stable convergence results near the near stall condition, while the SST-Helicity model improves the numerical stability of the near stall condition. The main reason is that the Helicity correction increases the turbulent viscosity, thus increasing the kinetic energy of the fluid within the turbulent boundary layer, which has a suppressive effect on the corner separation of the blade suction surface near the hub.

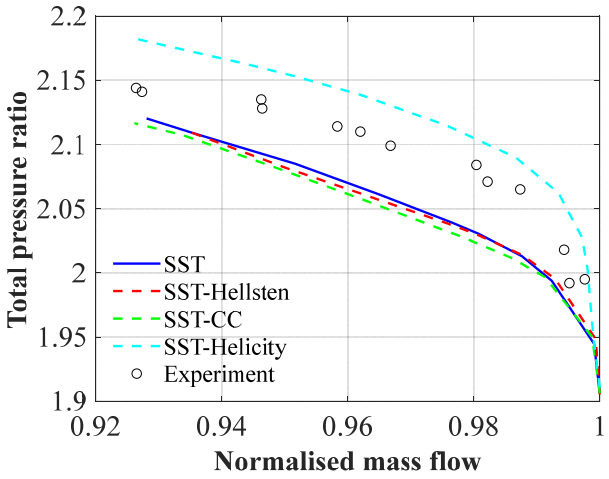

Figure 2. Total pressure ratio predictions from different SST models

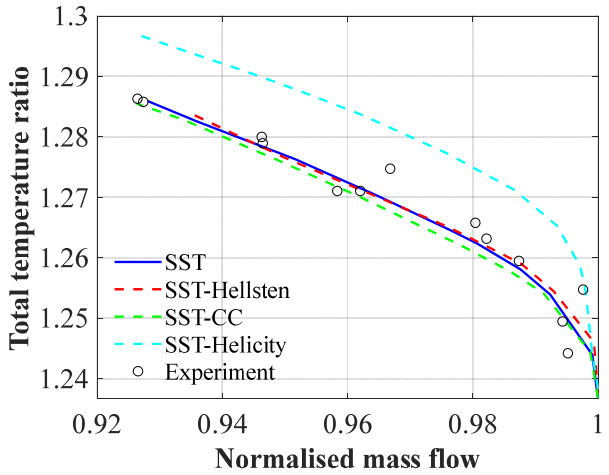

Figure 3. Total temperature ratio predictions from different SST models

In Fig. 4, SST-Helicity has the highest adiabatic efficiency; SST and SST-CC models are at the same level; SST-Hellsten has slightly lower adiabatic efficiency than the other models.

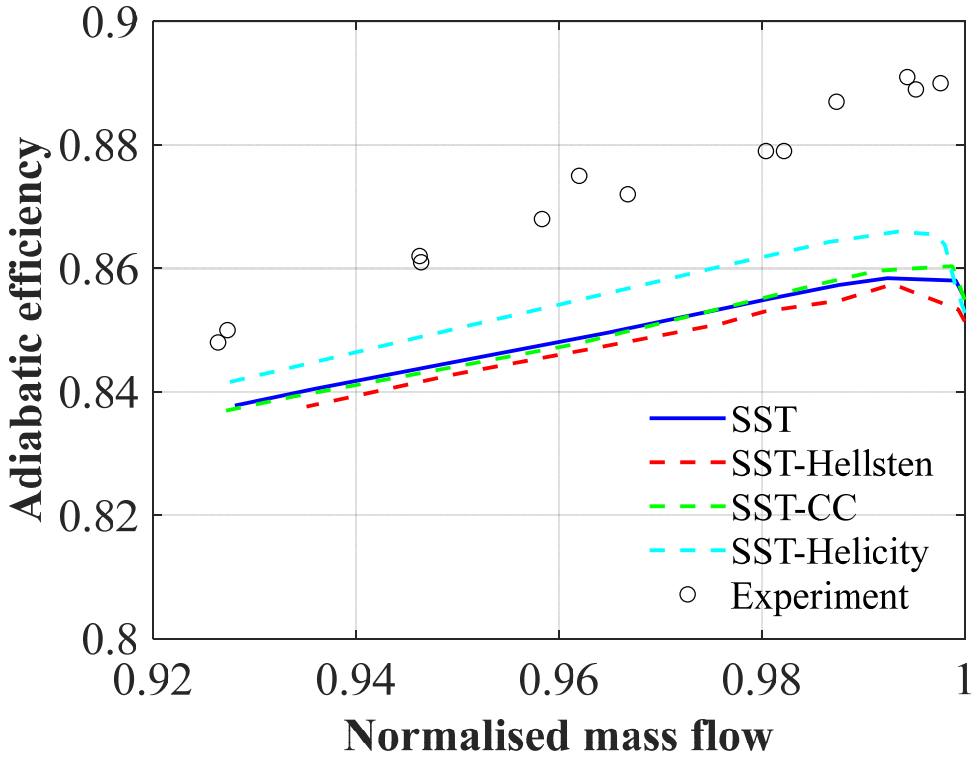

Figure 4. Adiabatic efficiency predictions of different modified SA models

In order to analyze the calculated results of various SST correction models in more detail and to reveal the reasons for the above overall parameter distributions, the spreading distributions of the compressor performance parameters at the outlet position for the 98% blockage flow condition and the near stall condition are shown in Fig. 5 and Fig. 6, respectively.

In the 98% blockage flow condition, the calculated total temperature and total pressure of the standard SST model, SST-CC and SST-Hellsten model are very close to each other and start to be significantly lower than the experimental values in the region above the 30% spread position; the total temperature and total pressure of the SST-Helicity model agree best with the experimental results, but the total pressure distribution below the 30% spread position is larger than the experimental values. greater than the experimental values. The standard SST model, SST-CC and SST-Hellsten model predict the corner separation near the root of the blade suction surface more accurately, while the SST-Helicity method suppresses the corner separation near the root of the blade, resulting in a larger total pressure near the root of the blade. In order to verify the above conjecture, Fig. 7 shows the distribution of the blade suction surface streamline bands for the SST-CC and SST-Helicity models at 98% blockage flow conditions. It can be seen that the range and intensity of flow separation near the root of the blade at the trailing edge of the SST-Helicity model is significantly weaker than that of the SST-CC model, and the flow lines are almost close to the blade suction surface and pass near the root of the blade, and some of the flow lines have a tendency to migrate toward the top of the blade; the SST-CC model has a significant surface layer separation at the position of the blade suction surface near the hub, which brings back the flow and significantly affects the flow in the radial direction of the flow.

In the near stall condition, the standard SST model, SST-CC and SST-Hellsten model agree better with the experimental results; the total temperature and pressure of the SST-Helicity model deviate more from the experimental results.

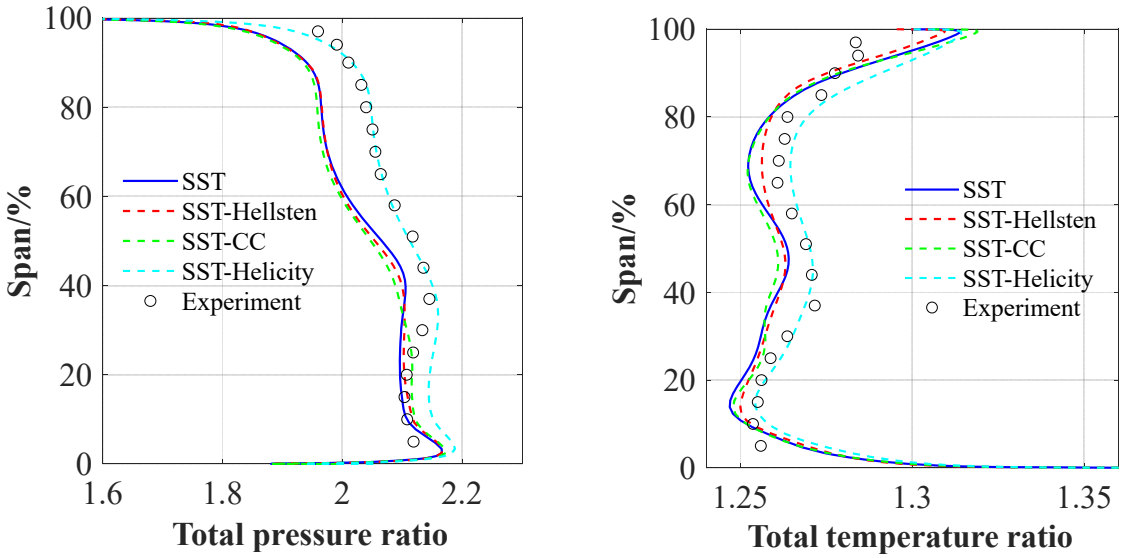

Figure 5. Spanwise distribution of performance parameters predicted with different SST models (98% choke mass flow)

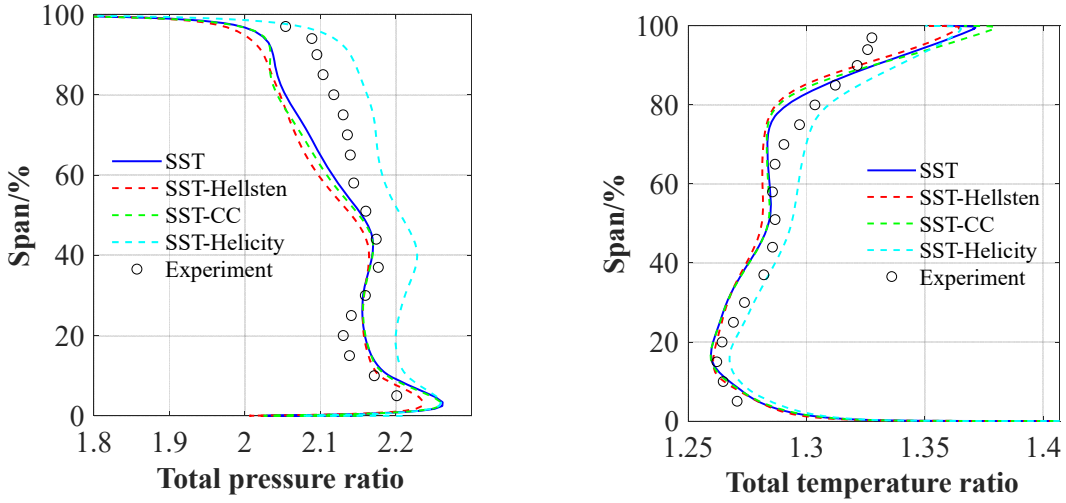

Figure 6. Spanwise distribution of performance parameters predicted with different SST models (Near stall condition)

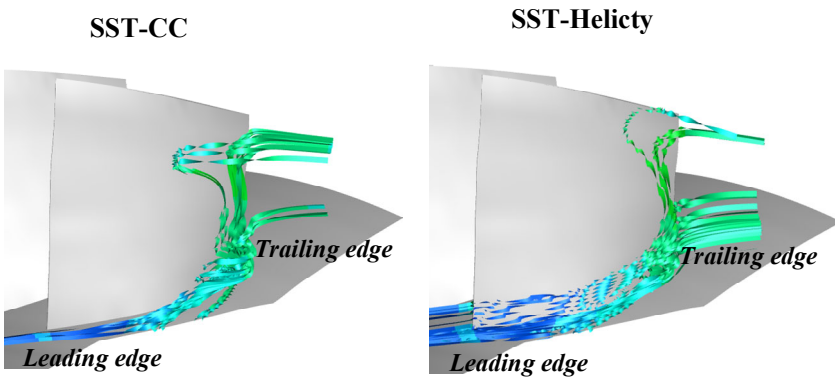

Figure 7. Streamtraces at suction surface

5. Conclusion

In this paper, the application of the rotation/curvature correction method of SST turbulence model to the flow simulation of Rotor37 is studied. Based on the simulation results of the compressor, the following conclusions are obtained:

(1) The SST-Helicity model takes into account the Energy Backscatter mechanism, which makes the corner separation suppressed. It can effectively improve the accuracy of model solution in the flow rate greater than 98% of the blockage flow rate; however, the total temperature and total pressure are over-predicted in the smaller flow rate condition.

(2) The total pressure and temperature obtained from the SST-CC and SST-Hellsten models are close to the standard SST model and have no optimization effect on the flow field solution of Rotor37.

The corner separation of suction surface of blade is one of the important causes of compressor total pressure loss. The Helicity correction can effectively improve the calculation accuracy of the SST model for the separation flow in this region. However, due to the complexity of tip leakage flow, the prediction error of all the modified models in this paper is still too large for the total pressure loss near the casing. Therefore, the flow mechanism and accurate modeling of tip leakage flow are worthy of further study.

Acknowledgments

The authors would like to thank Dr. Junbing LIU and Dr. Jingfan CHEN of the National University of Defense Technology for their helpful discussing on the data processing technology.

References

[1] Arima T, Sonoda T, Shirotori M, et al. A numerical investigation of transonic axial compressor rotor flow using a low reynolds number K-ε turbulence model[C].Turbo Expo: Power for Land, Sea, and Air. American Society of Mechanical Engineers, 1997, 78682: V001T03A017.

[2] Shabbir A, Zhu J, Celestina M. Assessment of three turbulence models in a compressor rotor[C]. Turbo Expo: Power for Land, Sea, and Air. American Society of Mechanical Engineers, 1996, 78729: V001T01A064.

[3] Yin Song, Jin Dong-hai, Zhu Fang, et al. Influence of turbulence models on simulation of a compressor[J]. Journal of Aerospace Power, 2010, 25(12): 2683-2689. (in Chinese)

[4] Liu Y, Yan H, Liu Y, et al. Numerical study of corner separation in a linear compressor cascade using various turbulence models[J]. Chinese Journal of Aeronautics, 2016, 29(3): 639-652.

[5] Suder K L, Celestina M L. Experimental and computational investigation of the tip clearance flow in a transonic axial compressor rotor[J]. 1996, 118(2): 218-229.

[6] Yutaka, MIYAKE, Takeo, et al. Numerical Simulation of the Effects of Coriolis Force on the Structure of Turbulence : 1st Report / Global Effect[J]. Transactions of the Japan Society of Mechanical Engineers.

[7] Wu H , Kasagi N . Effects of arbitrary directional system rotation on turbulent channel flow[J]. Physics of Fluids, 2004, 16(4):979-990.

[8] Kristoffersen, Reidar, Andersson, et al. Direct simulations of low-Reynolds-number turbulent flow in a rotating channel[J]. J. Fluid Mech, 1993.

[9] Nakabayashi K , Kitoh O . Low Reynolds number fully developed two-dimensional turbulent channel flow with system rotation[J]. Journal of Fluid Mechanics, 2006, 315(-1):1-29.

[10] Smits A J, Young S T B, Bradshaw P. The effect of short regions of high surface curvature on turbulent boundary layers[J]. Journal of Fluid Mechanics, 1979, 94(2): 209-242.

[11] So R M C, Mellor G L. Experiment on convex curvature effects in turbulent boundary layers[J]. Journal of Fluid Mechanics, 1973, 60(1): 43-62.

[12] Yang X, Tucker P G. Assessment of turbulence model performance: Large streamline curvature and integral length scales[J]. Computers & Fluids, 2016, 126: 91-101.

[13] Liu Y, Lu L, Fang L, et al. Modification of Spalart–Allmaras model with consideration of turbulence energy backscatter using velocity helicity[J]. Physics Letters A, 2011, 375(24): 2377-2381.

[14] Zhang Qian, Huang Xiu-quan, Wang Ding-xi. Evaluation of Different Spalart-Allmaras Turbulence Models for Turbomachinery Flow Field Analysis [J]. Journal of Propulsion Technology, 2022, 43(4): 200745. (in Chinese)

[15] Wang Zi-wei, Liu Dong-jian, Chen Ti. Numerical Simulation of the Rotating Stall Feature on a Single Stage Transonic Compressor[J]. PHYSICS OF GASES, 2021, 6(1): 30-37. (in Chinese)

[16] Hao Yan, Jiang Xiong, Qie Ming, et al. Numerical study on unsteady stator-rotor interaction in supersonic compressor[J]. Acta Aerodynamica Sinica, 2018, 36(5): 749-756. (in Chinese)

[17] Dunham J. CFD validation for propulsion system components (la validation CFD des organes des propulseurs)[R]. Advisory Group For Aerospace Research And Development Neuilly-Sur-Seine (France), 1998.

[18] Reid L. Performance of single-stage axial-flow transonic compressor with rotor and stator aspect ratios of 1.19 and 1.26, respectively, and with design pressure ration of 1.82[M]. NASA, Scientific and Technical Information Office, 1978.

[19] Menter F R. Two-equation eddy-viscosity turbulence models for engineering applications[J]. AIAA journal, 1994, 32(8): 1598-1605.

[20] Blazek J. Computational fluid dynamics: principles and applications[M]. Butterworth-Heinemann, 2015.

[21] Hellsten A . Some improvements in Menter's k-omega SST turbulence model[J]. AIAA Journal, 1998.